

Gas Phase $C_6H_6^-$ Anion: Electronic Stabilization by Opening of the Benzene Ring

Andriy Pysanenko, Ivo S. Vinklársek, Juraj Fedor, and Michal Fárník*

*J. Heyrovský Institute of Physical Chemistry,
Czech Academy of Sciences, Dolejškova 2155/3,
182 23 Prague, Czech Republic*

Stefan Bermeister

*Institut für Ionenphysik und Angewandte Physik,
Universität Innsbruck, Technikerstr. 25, A-6020 Innsbruck, Austria*

Vojtech Kostal, Tatiana Nemirovich, and Pavel Jungwirth†

*Institute of Organic Chemistry and Biochemistry, Czech Academy of Sciences,
Flemingovo nám. 2, 166 10 Prague 6, Czech Republic*

(Dated: September 28, 2022)

We present here results of experiments where low energy electrons are attached to medium-sized benzene clusters. Out of the various fragments observed in the mass spectrometer the most intriguing is the weak albeit unequivocal occurrence of a $C_6H_6^-$ moiety. Since the gas phase benzene radical anion is not electronically stable, we propose here – based on electronic structure calculation – that this moiety actually corresponds to linear structures formed by opening of the benzene ring via electron attachment.

I. INTRODUCTION

Benzene with its planar hexagonal form of D_{6h} symmetry represents one of the most iconic structures in chemistry. An interesting question is how this structure changes upon varying its charge state. The benzene radical cation, $C_6H_6^+$, is Jahn-Teller active and thus has two structural forms – the compressed and elongated rings. They are energetically very close to each other and their abundance depends on the elementary environment of the cation (ref). Even more interesting is the benzene dication, $C_6H_6^{2+}$, which has a number of stable isomers with the most stable structure being the pyramidal one with a C_5H_5 base and a CH group at the apex (ref). Nonetheless, independent from these structural peculiarities, both the cation and dication are directly observed, e.g., in the standard electron impact mass spectra of benzene.

The situation is very different for the benzene radical anion, $C_6H_6^-$, which has not been detected in the isolated form. The reason is that anionic states of benzene are embedded in the continuum and the electron thus undergoes autodetachment on an ultrafast timescale. For example, the lowest anion state, which is a e_{2u} shape resonance, lies 1.12 eV above the neutral benzene and its electronic width of 0.12 eV corresponds to autodetachment lifetime of XXX fs. Upon ring distortion the energy of this resonant state slightly decreases (ref) however, no configuration has been found where this anion state is below the neutral, i.e., the gas phase radical anion is not electronically stable. However, this situation

changes dramatically upon solvation. The benzene anion $C_6H_6^-$ is electronically stabilized and readily observed in solvents, e.g., in liquid ammonia [1] and in ammonia clusters[2].

The above considerations govern the outcome of reactions of benzene-containing species with free electrons. For a gas phase benzene molecule, the formation of low-lying shape resonances leads merely to a considerable vibrational excitation [3]. For high lying core-excited resonances, the dissociative electron attachment channel opens, which leads to hydrogen abstraction; the $C_6H_5^-$ cross section peaks at 8 eV with a shoulder up to 10 eV [4]. Upon electron attachment to large benzene clusters at low electron energies (~ 0.3 eV), benzene cluster anions $(C_6H_6)_n^-$ were detected for sizes $n \geq 53$ [5]. This was interpreted as formation of a solvated electron in benzene, which was supported by photoelectron spectroscopy. No negatively charged benzene clusters were observed for smaller sizes at these low electron energies. However, at much higher electron energies of hundreds of eV, cluster anions with $n \leq 52$ (down to $n = 2$) were observed through fragmentation of large $(C_6H_6)_n^-$ clusters. In this paper we report the first observation of a stable isolated $C_6H_6^-$ anion with lifetime is longer than ten microseconds and we attribute its formation to the opening of the benzene ring and formation of chain-like structures.

II. EXPERIMENT

We generated benzene clusters by a continuous supersonic expansion of a benzene vapor with an argon buffer gas. The gas was expanded through a conical nozzle (90 μ m diameter, 30° full opening angle, and 2 mm

* michal.farnik@jh-inst.cas.cz

† pavel.jungwirth@uochb.cas.cz

length), which was attached to the benzene containing reservoir placed in the source vacuum chamber. The reservoir temperature and nozzle temperature of $T_R \approx 300$ K and $T_0 = 333$ K, respectively, were kept constant by independent heating. The Ar stagnation pressure was $P_0 = 3$ bar, i.e., the benzene concentration in the gas mixture with Ar was about 5%. These expansion conditions result in $(C_6H_6)_N$ with the mean neutral cluster size of $\bar{N} \approx 300$. The cluster size was determined in our recent pickup experiments [6].

In our present case of relatively large neutral $(C_6H_6)_N$ clusters, the measured cluster ion fragment (positively or negatively charged) mass spectra do not fully reflect the neutral cluster size distributions. First, they suffer from the cluster fragmentation upon ionization, and second, our time-of-flight mass spectrometer in perpendicular arrangement has a limited mass range ($m/z \approx 600$), within which the spectra can be obtained without any mass discrimination. The pickup experiment represents a more reliable methods to determine the mean neutral cluster size. A detailed discussion can be found in Ref. [6]. Nevertheless, in the present investigation of the negatively charged benzene clusters, we concentrate on the mass region below $m/z \leq 700$.

After the expansion the clusters passed through a skimmer followed by three differentially pumped vacuum chambers, and they were detected in a fourth one by a reflectron time-of-flight mass spectrometer (TOF), first implemented and described elsewhere [7, 8]. It can detect either positive ions [7, 8], or it can work in the negative ion mode [9, 10] employed in the present experiments. The clusters are ionized by an electron beam pulsed at a frequency of 10 kHz. The pulse width was 5 μ s and extraction and acceleration voltages of 4 keV and 8 keV, respectively, were applied with a delay of 0.1 μ s to prevent any unwanted ionization with electrons accelerated by the extraction voltage. After the flight path of approximately 95 cm in the reflectron TOF, the ions were detected with a microchannel plate detector and the mass spectra were recorded. The electron energy was scanned between 0 and 12 eV in steps of 0.2 eV to obtain electron energy dependent mass spectra and an energy-dependent negative ion yield. However, due to the very low abundance of the $(C_6H_6)_n^-$ ions some of the presented spectra were recorded for a very long time (several repeated days) at a single electron energy of 8 eV, where the maximum of $(C_6H_6)_n^-$ ion signal occurred. The energy scale calibration was done using the 4.4 eV and 8.2 eV resonances in the electron attachment of CO_2 molecules.

III. CALCULATIONS

All electronic structure calculations of the $C_6H_6^-$ structures and their neutral counterparts were carried out using the ORCA 5.0.1 program package [11]. Geometries of the anionic structures were first pre-optimized at the second-order Møller-Plesset perturbation theory

level (MP2) [12, 13] employing the cc-pVDZ basis set and then evaluated at the complete active space self-consistent field [14] (CASSCF) level using cc-pVTZ basis set [15, 16]. Note that the CASSCF calculation always used MP2-based natural orbitals (NO) as an initial guess calculated with the same basis set. Size of the active space was chosen based on the NO analysis such that orbitals with occupation numbers between 0.05 and 1.95 were considered as the active ones. This resulted in using the CASSCF-(7-6) method for the anionic structures and CASSCF-(6-6) for the neutral ones.

Final single-point energies were the calculated at complete active space perturbation theory [14] (CASPT2) with the aug-cc-pVDZ basis starting again from natural orbitals calculated at the MP2/aug-cc-pVDZ level. Vertical detachment energies (VDE) were subsequently obtained as the difference between the single-point energy of the anionic and neutral structures at the geometry of the anionic one. Additional benchmarks concerning convergence of the VDE with respect to the basis set and size of the active space are presented in the SI.

IV. RESULTS

A. Mass Spectra

Fig. 1 shows the mass spectrum of negatively charged benzene clusters after the electron attachment to the pure $(C_6H_6)_N$ clusters. The negative ions have extremely low intensities, therefore the spectrum was recorded and accumulated for a long time at a constant electron energy of 8 eV. This energy roughly corresponds to the maximum signal for the $(C_6H_6)_n^-$ cluster ions as shown below. The major peaks in the spectrum correspond to the $(C_6H_6)_{n-1}C_6H_5^-$ and $(C_6H_6)_n^-$ series. For the first members of the series $n = 1$ the fragment $C_6H_5^-$ ion at $m/z = 77$ is slightly dominating over $m/z = 78$, however, for $n \geq 2$ $(C_6H_6)_n^-$ dominate over the neighboring $(C_6H_6)_{n-1}C_6H_5^-$ fragment. Apart from these, there is a weaker series starting at $m/z = 110$ (orange triangles) assigned to $(C_6H_6)_nO_2^-$ due to a small oxygen impurity deposited in the clusters from the vacuum background, which is discussed below. Finally, there is a very weak series of mass peaks displaced by $\Delta m/z = -15$ from the $(C_6H_6)_n^-$ peaks (green diamonds) tentatively assigned to $(C_6H_6)_{n-1}C_5H_2^-$, i.e., dissociation of CH_3 from benzene clusters upon the electron attachment.

First, we discuss the $(C_6H_6)_nO_2^-$ series with oxygen impurity. The presence of the oxygen containing clusters may be surprising since the background pressure in all chambers, which the clusters pass through, is in the region 10^{-6} - 10^{-9} mbar and we do not see any evidence for the oxygen present on the benzene clusters in the positively charged ion spectrum. The expected amount of oxygen picked up by the $(C_6H_6)_n^-$ clusters from the background is very small. We can make the following estimate – from other experiments [6], we know the mean

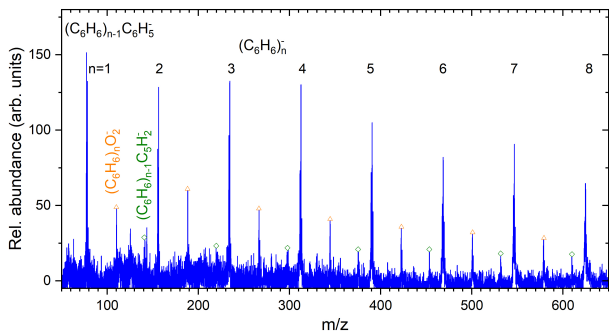


FIG. 1. The mass spectrum of negatively charged clusters after 8 eV electron attachment to $(\text{C}_6\text{H}_6)_n$ clusters. The major series are $(\text{C}_6\text{H}_6)_{n-1}\text{C}_6\text{H}_5^-$ and $(\text{C}_6\text{H}_6)_n^-$. Further series indicated: $(\text{C}_6\text{H}_6)_n\text{O}_2^-$ (orange triangles) due to an oxygen impurity, and $(\text{C}_6\text{H}_6)_{n-1}\text{C}_5\text{H}_2^-$ (green diamonds).

size of our neutral $(\text{C}_6\text{H}_6)_N$ clusters of $\bar{N} \approx 300$, which corresponds to the mean cluster radius of 2.2 nm. The clusters fly about 1.5 m in the vacuum of 10^{-6} mbar or lower. From this we deduce that the uptake probability of a single molecule by the average cluster is ≤ 0.5 , i.e., less than half of the clusters can pick up an O_2 molecule, and the uptake of more than one molecule is probable only for the largest, less abundant, clusters. However, oxygen molecules have large electron attachment cross sections [17]. Thus, the electrons attached temporarily to benzene clusters in a metastable state can be stabilized by the oxygen molecule and we may thus see the oxygen containing clusters in the negative ion spectrum despite their low abundance. To check this hypothesis, we deliberately doped the $(\text{C}_6\text{H}_6)_N$ clusters with more O_2 molecules by filling the oxygen gas into a pickup chamber at the pressure of 1×10^{-4} mbar increasing the mean number of collisions of an average cluster with O_2 molecules about 10-times, i.e. each cluster should collide with several (~ 5) O_2 molecules. This experiment resulted in the spectrum completely overwhelmed by $(\text{C}_6\text{H}_6)_n\text{O}_2^-$ series while the $(\text{C}_6\text{H}_6)_n^-$ intensities remained unchanged by the oxygen doping.

As outlined already in the introduction, the most interesting observation is the appearance of the $(\text{C}_6\text{H}_6)_n^-$ ions and of the C_6H_6^- monomer in particular. However, one has to be careful here, since there are isotope contributions from the $(\text{C}_6\text{H}_6)_{n-1}\text{C}_6\text{H}_5^-$ ions at the corresponding $(\text{C}_6\text{H}_6)_n^-$ ion masses. Therefore, we show the spectrum of Fig. 1 in more details in Fig. 2, where the orange horizontal lines correspond to the calculated isotope contribution to the $(\text{C}_6\text{H}_6)_n^-$ ion peaks based on the $(\text{C}_6\text{H}_6)_{n-1}\text{C}_6\text{H}_5^-$ abundances. The isotope contribution clearly cannot account for the entire intensity of the $(\text{C}_6\text{H}_6)_n^-$ peaks.

Nevertheless, we have made another test with deuterated benzene C_6D_6 to prove the presence of the $(\text{C}_6\text{H}_6)_n^-$ ions including the monomer. Figure 3 proves the C_6D_6^- ion peak unambiguously and shows that the isotope contribution of C_6D_5^- at $m/z = 83$ is small. Thus, all the

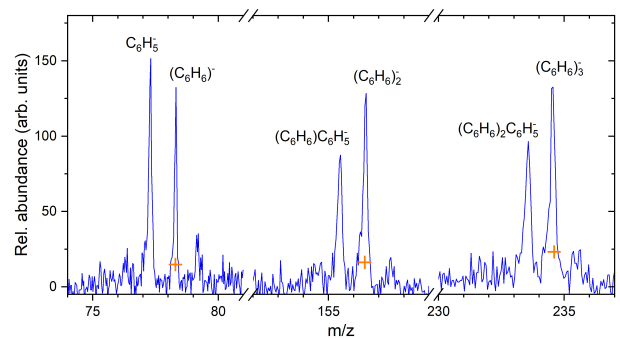


FIG. 2. The detail of mass spectrum of negatively charged $(\text{C}_6\text{H}_6)_n^-$ clusters shown in Fig. 1. Horizontal lines show the isotope contribution to the $(\text{C}_6\text{H}_6)_n^-$ ion peaks based on the $(\text{C}_6\text{H}_6)_{n-1}\text{C}_6\text{H}_5^-$ abundances.

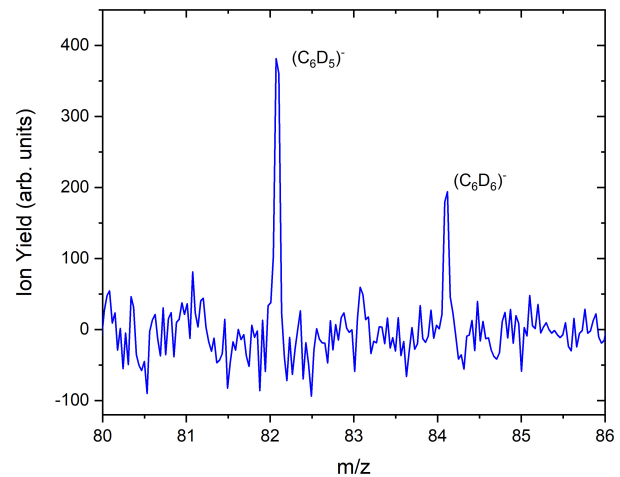


FIG. 3. The mass spectrum of negatively charged deuterated $(\text{C}_6\text{H}_6)_n$ clusters showing that the isotope contribution of C_6D_5^- at $m/z = 83$ is relatively small compared to the C_6D_6^- ion peak.

experimental evidence proves unambiguously the generation of $(\text{C}_6\text{H}_6)_n^-$ ion by electron attachment to large $(\text{C}_6\text{H}_6)_N$ clusters.

B. Energy dependence

To explore the origin of the $(\text{C}_6\text{H}_6)_n^-$ ions further, we show the energy-dependent ion yields of these ions in Figure 4. Note that the top spectrum (green circles) shows the dependence for C_6D_6^- ion offset by a factor of 10 in the y-axis. The $(\text{C}_6\text{H}_6)_n^-$ and $(\text{C}_6\text{H}_6)_{n-1}\text{C}_6\text{H}_5^-$ ion yields are shown by the bottom red squares and blue diamonds, respectively. The ions exhibit very low intensities and thus we have integrated several $n = 1-4$ ion yields to obtain energy dependencies with somewhat reasonable signal-to-noise ratio. All the spectra exhibit a maximum around 8 eV. Despite the low signal, the peak position agrees well with the previously measured disso-

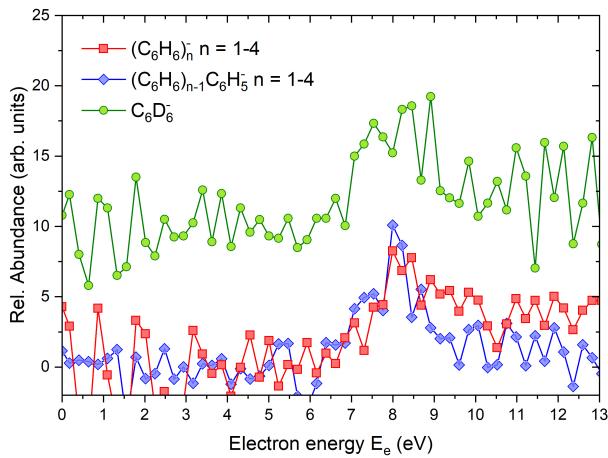


FIG. 4. The energy-dependent ion yield of different ions: $C_6D_6^-$ (green circles) is offset by 10 in y-axis; $(C_6H_6)_n^-$ (red squares) and $(C_6H_6)_{n-1}C_6H_5^-$ (blue diamonds) ion yields have been integrated for $n = 1-4$ to obtain reliable energy dependencies.

ciative electron attachment (DEA) spectrum of benzene yielding $C_6H_5^-$, where a single peak at 8 eV with a weak shoulder extending to 10 eV was observed [4].

C. Computational Results

We consider six linear structures that can form upon benzene ring opening due to the electron attachment – a direct product of the ring opening carrying one hydrogen on each carbon atom (structure 1 in Figure 5) and five structures with one shifted hydrogen atom (structures 2-5 in Figure 5). Geometries of these radical anions were optimized according to the protocol described above and their energies were then obtained at the CASSCF-(7-6)/aug-cc-pVDZ level. These energies, referenced to the total energy of neutral benzene at the CASSCF-(6-6)/aug-cc-pVDZ level, are presented in Figure 5. It can be seen from this figure that energies of all the structures lie only up to 5 eV above the energy of neutral benzene, rendering the ring-opening event thermodynamically feasible as the energy of the incident electrons is about 8 eV.

Table I presents VDEs of the six linear structures. Unlike the benzene radical anion which is electronically unstable in the gas phase (having a non-negative VDE) [1], it can be seen from Table I that all the considered linear radical anion structures are electronically stable, possessing sizable negative VDEs.

V. DISCUSSION

The mass spectra in Figs. 2 and 3 show that the $C_6H_6^-$ and $(C_6H_6)_n^-$ radical anions are generated in the process of attachment of slow (~ 8 eV) electrons to large

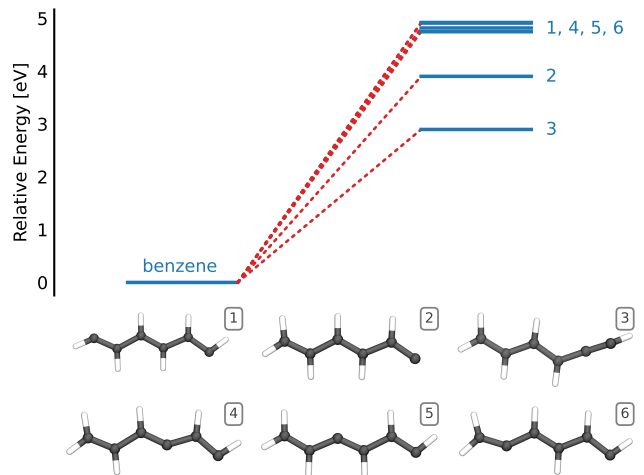


FIG. 5. Total electronic energies (top) of the proposed linear structures (bottom) relative to the energy of neutral benzene.

Structure	VDE [eV]
1	-1.603
2	-2.926
3	-2.355
4	-1.453
5	-1.520
6	-1.610

TABLE I. Calculated VDEs of the six linear structures from Figure 5.

($\bar{N} \approx 300$) benzene clusters. Their abundance is low, yet their appearance is unambiguous. Experiments with the deuterated benzene provided further evidence that the monomeric signal corresponds, indeed, to the $C_6H_6^-$ radical anion and not just to the isotope contribution of $C_6H_5^-$, which is quite common product of the DEA process. The formed negative anions must be stable at least on the time scale of their flight time in our TOF spectrometer, which is about 10 μs for the $C_6H_6^-$ monomer and even longer for $(C_6H_6)_n^-$ clusters.

Large $(C_6H_6)_n^-$ cluster anions with $n \geq 53$ were reported to be formed in abundance via generation of the solvated electron in Ref. [5]. We cannot compare yields of our smaller $(C_6H_6)_n^-$ clusters to the yields of the large ones, since such large clusters cannot be detected in our TOF spectrometer due to its perpendicular arrangement. All the clusters generated in supersonic expansions attain essentially the same velocity with a very narrow distribution. When the ionized clusters are extracted in the TOF region perpendicularly to the beam velocity, they keep the component of velocity parallel to the beam, and thus the heavier ones, which spend longer time in the TOF region, can escape the detection. We can partly compensate for that effect by applying a deflection voltage against the beam direction, however, we still cannot detect clusters of $m/z \geq 4000$. A more detailed discus-

sion of this effect in out TOF can be found elsewhere [18].

We have measured the energy dependent ion yields, as presented in Fig. 4, to shed more light onto the origin of the $(\text{C}_6\text{H}_6)_n^-$ clusters. Despite the low signal-to-noise ratio, results shown in Figure 4 suggest that all observed negative ions are generated by attachment of an electron with energy around 8 eV. Note that this energy is also compatible with the DEA process of isolated benzene molecule yielding C_6H_5^- . Thus DEA of benzene may be the initial step in the generation of both

$(\text{C}_6\text{H}_6)_{n-1}\text{C}_6\text{H}_5^-$ and $(\text{C}_6\text{H}_6)_n^-$ ions. In the latter case, caging of the departing hydrogen may lead to $(\text{C}_6\text{H}_6)_n^-$ ions, as observed in our earlier studies [10, 19, 20]. However, the monomeric benzene radical anion cannot be formed as it is electronically unstable. Instead, ring-opening is proposed here as the mechanism leading to the mass spectrometric detection of electronically stable linear C_6H_6^- ion structures. Present calculations show that, indeed, multiple linear structures of C_6H_6^- , which are electronically stable, can be formed by attachment of an electron with 8 eV kinetic energy, rendering the ring-opening mechanism viable.

-
- [1] V. Kostal, K. Brezina, O. Marsalek, and P. Jungwirth, Benzene radical anion microsolvated in ammonia clusters: Modeling the transition from an unbound resonance to a bound species, *J. Phys. Chem. A* **125**, 5811 (2021).
- [2] A. Pysanenko, S. Bergmeister, P. Scheier, and M. Fárník, Stabilization of benzene radical anion in ammonia clusters, *Phys. Chem. Chem. Phys.* **XXX**, XXX (2022).
- [3] M. Allan, R. Čurík, and P. Čársky, Coupling of electronic and nuclear motion in a negative ion resonance: Experimental and theoretical study of benzene, *J. Chem. Phys.* **151**, 064119 (2019).
- [4] H.-P. Fenzlaff and E. Illenberger, Low energy electron impact on benzene and the fluorobenzenes. formation and dissociation of negative ions, *Int. J. Mass Spec. Ion Proc.* **59**, 185 (1984).
- [5] M. Mitsui, A. Nakajima, K. Kaya, and U. Even, Mass spectra and photoelectron spectroscopy of negatively charged benzene clusters $(\text{benzene})_n^-$ ($n = 53-124$), *J. Chem. Phys.* **115**, 5707 (2001).
- [6] I. S. Vinklárěk, A. Pysanenko, E. Pluhařová, and M. Fárník, Uptake of hydrogen bonding molecules by benzene nanoparticles, *J. Phys. Chem. Lett.* **13**, 3781 (2022).
- [7] J. Lengyel, A. Pysanenko, J. Kočíšek, V. Poterya, C. Pradzynski, T. Zeuch, P. Slavíček, and M. Fárník, Nucleation of mixed nitric acid-water ice nanoparticles in molecular beams that starts with a hno_3 molecule, *J. Phys. Chem. Lett.* **3**, 3096 (2012).
- [8] J. Kočíšek, J. Lengyel, and M. Fárník, Ionization of large homogeneous and heterogeneous clusters generated in acetylene-ar expansions: Cluster ion polymerization, *J. Chem. Phys.* **138**, 124306 (2013).
- [9] J. Lengyel, J. Kočíšek, M. Fárník, and J. Fedor, Self-scavenging of electrons in $\text{fe}(\text{co})_5$ aggregates deposited on argon nanoparticles, *J. Phys. Chem. C* **120**, 7397 (2016).
- [10] J. Kočíšek, A. Pysanenko, M. Fárník, and J. Fedor, Microhydration prevents fragmentation of uracil and thymine by low-energy electrons, *J. Phys. Chem. Lett.* **7**, 3401 (2016).
- [11] F. Neese, Software update: The ORCA program system—Version 5.0, *Wiley Interdisciplinary Reviews: Computational Molecular Science*, e1606 (2022).
- [12] C. Møller and M. S. Plesset, Note on an Approximation Treatment for Many-Electron Systems, *Physical Review* **46**, 618 (1934).
- [13] M. Head-Gordon, J. A. Pople, and M. J. Frisch, MP2 energy evaluation by direct methods, *Chemical Physics Letters* **153**, 503 (1988).
- [14] B. O. B. r. O. Roos, R. Lindh, P. A. Malmqvist, V. Veryazov, and P.-O. Widmark, *Multiconfigurational quantum chemistry* (John Wiley & Sons Inc (Verlag), 2016).
- [15] T. H. Dunning, Gaussian basis sets for use in correlated molecular calculations. I. The atoms boron through neon and hydrogen, *The Journal of Chemical Physics* **90**, 1007 (1989).
- [16] R. A. Kendall, T. H. Dunning, and R. J. Harrison, Electron affinities of the first-row atoms revisited. Systematic basis sets and wave functions, *The Journal of Chemical Physics* **96**, 6796 (1998).
- [17] Y. Itikawa, Cross sections for electron collisions with oxygen molecules, *J. Phys. Chem. Ref. Data* **38**, 1 (2009).
- [18] J. Lengyel, A. Pysanenko, V. Poterya, J. Kočíšek, and M. Fárník, Extensive water cluster fragmentation after low energy electron ionization, *Chem. Phys. Lett.* **612**, 256 (2014).
- [19] J. Lengyel, M. Ončák, J. Fedor, J. Kočíšek, A. Pysanenko, M. K. Beyer, and M. Fárník, Electron-triggered chemistry in $\text{hno}_3/\text{h}_2\text{o}$ complexes, *Phys. Chem. Chem. Phys.* **19**, 11753 (2017).
- [20] J. Lengyel, A. Pysanenko, and M. Fárník, Electron-induced chemistry in microhydrated sulfuric acid clusters, *Atmos. Chem. Phys.* **17**, 14171 (2017).